WATER-TO-CEMENT RATIO PREDICTION USING ANNS FROM NON-DESTRUCTIVE AND CONTACTLESS MICROWAVE MEASUREMENTS

U. C. Hasar [†]

Department of Electrical and Electronics Engineering
Ataturk University
Erzurum 25240, Turkey

G. Akkaya, M. Aktan, and C. Gozu [‡]

Department of Industrial Engineering
Ataturk University
Erzurum 25240, Turkey

A. C. Aydin

Department of Civil Engineering
Ataturk University
Erzurum 25240, Turkey

Abstract—In concrete industry, there is a need for water-to-cement ratio (w/c) estimation of cement-based materials since the w/c ratio of cement mixtures is typically given at the batch plant, and this ratio, sometimes, is deliberately changed to have a more workable cement mixture. To meet the requirements of accurate w/c ratio determination of cement-based materials, in this research paper, we propose an artificial neural network approach for w/c ratio estimation of these materials using free-space non-contact reflection and transmission measurements of mortar specimens with w/c ratios of 0.40, 0.45, 0.50, 0.55 and 0.60. We have tested the network and observed less than 5 percent difference between the estimated and known values of w/c = 0.50.

Corresponding author: U. C. Hasar (ugurcem@atauni.edu.tr).
[†] Also with Department of Electrical and Computer Engineering, Binghamton University, Binghamton, NY 13902, USA.
[‡] C. Gozu is also with School of Business, State University of New York at Albany, Albany, NY 12222, USA.

1. INTRODUCTION

Cement-based composites are multiphase, exceedingly complex heterogeneous materials, and cement-based composite is one of the principal materials for structures. The heterogeneity and properties of cement-based composite are mostly concerned with the hydration. Hydration, the chemical reaction between water and ingredients of cement, is one of the most important properties of its strength gain process. This property of hydration is caused by volume change of hydrated cement, varying hydration rate through the cement-based composite and time dependency of strength gain. One of the main reasons of strength gain is the mechanical properties of cement-based composites. The mechanical properties of cement-based material is needed by designers for stiffness and deflections evaluation and is a fundamental property required for the proper modeling of its constitutive behavior and for its proper use in various structural applications. For this reason, determination of mechanical properties of cement-based composite has become very important from a design point of view [1, 2].

General methods used in civil engineering for characterizing the mechanical properties of cement-based materials are either to prepare a sample with the same mix proportions in the lab, or to drill a sample from the structure, and then test in the lab. The sample preparation method does not reflect the actual measurement of interest since the sample in the lab and the materials cast in the field are not cured the same [3]. The sample removal method is clearly harmful to the overall structure as a result of removing of a test sample (removed sample). The test techniques used for both methods are destructive [4] because the sample is damaged and cannot be reused in future. Several non-destructive evaluation (NDE) techniques have been applied to quality assessment, mixture content evaluation, and monitoring the internal integrity (voids, cracks, degradation, etc.) of cement-based materials [5]. These techniques are ultrasound, infrared thermography, radiography, ground-penetrating radar, and microwaves. Compared to other NDE techniques, microwaves are not hazardous, scatter little compared to acoustic waves, low in cost compared to radioactive methods, noncontact (microwave sensor-antenna), and with good spatial resolution and superior penetration in nonmetallic materials [6, 7].

A strong correlation was observed between the microwave near-field reflection measurements and the state and degree of hydration (a chemical reaction and binding of water and cement molecules), water-to-cement ratio (w/c), sand-to-cement ratio (s/c), coarse

aggregate-to-cement ratio (ca/c), and compressive strength of cement-based materials [1, 3, 8, 9]. However, these measurements have some disadvantages for investigation of these materials. First, they require contact or close proximity probing with the material under test [7] and a well-positioned antenna or probe to reduce the diffraction at the interface. Second, the dielectric properties of materials in the near-field of an antenna are known to influence the antenna beam. Finally, the numerical modelling of wave-material interaction by near-field techniques is relatively complex [7, 10, 11].

Far-field microwave measurements have also shown a great potential for the investigation of cement-based materials [7, 11–16]. These techniques are contact-free methods that deal with only the dominant excitation mode and also allow plane wave assumption for modelling. This assumption considerably simplifies the numerical model for studying wave propagation in concrete structures [7, 13–16]. These techniques enable large area coverage, are very suitable for remote sensing [11], and do not necessitate special sample preparation [17]. The feasibility of a robust, free-space, and far-field microwave NDE technique for imaging cement-based materials via numerical simulations and experiments [7] and for inspecting reinforced concrete structures [12] was investigated. The dependencies of microwave far-field reflection and transmission properties of hardened mortar and concrete structures [13, 14] and young mortar structures [15] on water-to-cement ratio (w/c), preparation, and curing conditions have also been reported. It has been shown that the speed of hydration process depends on various sides of cement-based materials as well as the w/c ratio and curing conditions [13]. In another study [16], it has also been demonstrated that the effect of various sides of these materials on transmission properties and that a varying electrical property depending on height should be used for hardened cement-based materials in predicting the channel properties in propagation-related researches. However, to the best knowledge of the authors, the correlation between far-field transmission properties of young cement-based materials (materials which are 2–3 days old) and water-to-cement ratio (w/c) has not yet been investigated. This study is important since, in practice, the w/c ratio is the key factor that influences the strength, which is an indication of the robustness of structures such as buildings to a possible earthquake, of fully compacted concrete the most [4]. The w/c ratio of cement mixtures is typically given at the batch plant. Neural network modeling approach outperforms the other given models in terms of prediction capability. In addition, it allows fast inversion of the data in terms of the desired unknown (w/c ratio). Thus, it can be used as a viable

tool for modeling or estimation of the w/c ratio of cement-based materials. The motivation of this research paper is to demonstrate the applicability of reflection and transmission far-field measurements for w/c estimation of cement samples and evaluate whether far-field transmission measurements or reflection measurements are suitable and better for w/c estimation.

2. MIXTURE PROPORTIONS OF SPECIMENS

Mortar specimens with different w/c ratios between 0.40–0.60 with 0.05 w/c ratio increment were analyzed in Section 4 for the w/c ratio estimation from reflection and transmission properties. The percentages of raw materials of these specimens are given in [15]. The cement used in the experiment is the ASTM Type I normal Portland Cement, 100% of the sand mass consists of particles less than 4 mm in diameter. Well-graded, quartzite, natural sand is used. The sand complies with the requirements of ASTM C-33 [18]. The absorption capacity is 0.1% and its specific gravity (relative density) at saturated surface dry condition is 2.72. The absorption capacity is determined by bulk specific gravity on SSD and dry basis [19].

The thickness of samples is chosen in such a way that early transmission measurements of young mortar specimens can be detected. According to the previous study [14], optimum thickness of samples was selected as 100 mm after some transmission measurements. The lateral dimensions of the samples are 150 mm × 150 mm. During measurements, the temperature and relative humidity for curing conditions were kept between 28–32°C and 50–60%, respectively, at ordinary laboratory room conditions.

3. MEASUREMENT SETUP AND CALIBRATION PROCEDURE

The measurement set-up and the calibration procedure for reflection and transmission properties of young mortar specimens were given in [15]. The set-up measures amplitudes of reflection and transmission coefficients from electric field strengths of incident, reflected, and transmitted waves. It is composed of rectangular waveguide sections, a microwave source, a rotary attenuator, two directional couplers, two antennas, and three diode detectors. The source operates between 8.2–12.5 GHz. Its output power is approximately 10 mW at X-band. This source level is suitable and applicable for most microwave nondestructive applications [20].

The signal from the source is modulated by a 1 kHz signal to measure amplitude-modulated reflected and transmitted signals by a simple reflectometer and an attenuation-meter. The simple reflectometer consisting of two square-law detectors and two couplers is constructed to measure the reflection coefficient. The attenuation-meter measures the transmission coefficient and consists of two square-law detectors and the first coupler.

A rotary attenuator is used to change the level of the incident signal and to decrease the level of reflected signal at the source. The rotary attenuator is a FLANN 16110 precision attenuator with 0 to 60 dB attenuation range and 0.1 dB reading accuracy. We used FLANN 16131 multihole directional couplers. These couplers operate at 8.2–12.5 GHz, have a minimum 40 dB directivity, and a coupling of 20 dB. Standard gain horn antennas are used for matching impedances of air and waveguide aperture. These antennas have an aperture of 60.5 mm×45 mm, a gain of approximately 15 dB, and a half-power beamwidth of 33° at X-band.

For measurements of reflection and transmission properties, the samples were placed between the horn antennas according to: a) the plane wave condition is fulfilled; b) the placement of the center of samples exactly matches to the center of the horn antennas; c) the aperture of the antennas is positioned to be parallel to the transverse dimension of the samples; d) the minimum amount of wave is scattered by the edges of the sample; e) the maximum amount of the incident signal is received by the receiving antenna when there is no sample between the antennas; f) samples are placed exactly at the middle of the distance between antennas [15].

For calibration of measurement set-up, we utilized reflection measurement of a metal (copper) plate exactly at the position where front face of the specimen is located (reference for reflection measurements) and transmission measurement when there is no sample present between horn antennas (reference for transmission measurements) [15]. For more details on the measurement set-up and the libration procedure, the reader can refer to [15].

4. WATER-TO-CEMENT RATIO ESTIMATION USING ANNS

For validation of the w/c ratio estimation from reflection and transmission free-space measurements of cement materials by the proposed method, we utilize the hourly measurements of reflection and transmission properties of young mortar specimens with different w/c ratios between 20–30 hours and 44–54 hours at 8.5 GHz in [15]. The
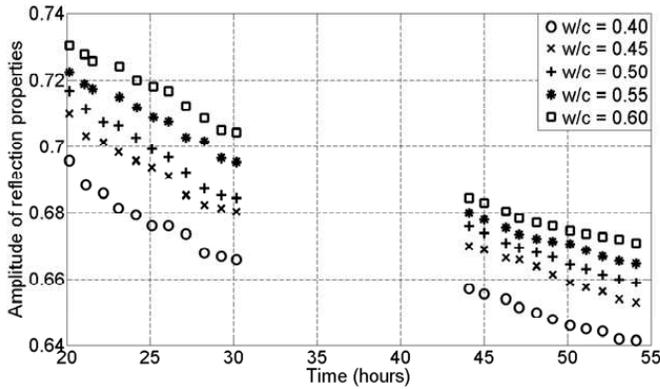
Figure 1. Measured amplitude of free-space reflection measurements over time. The measurement data is obtained from [15].
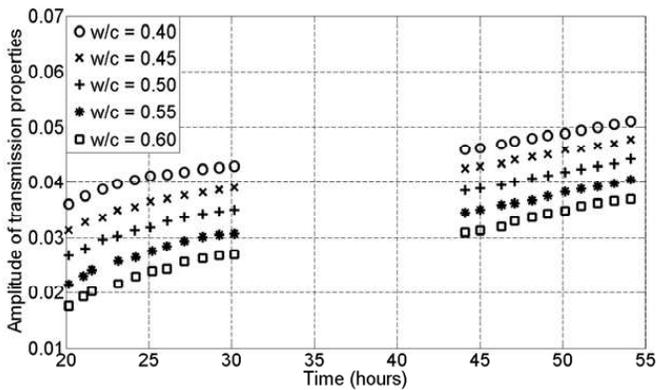

Figure 2. Measured amplitude of free-space transmission measurements over time. The measurement data is obtained from [15].

measurements of these properties are shown in Figs. 1 and 2. In the estimation of w/c ratio of these specimens using these measurements, in this research paper, we utilize artificial neural networks (ANNs) since, once trained by an appropriate set of measurement data, they allow fast inversion of the data in terms of the desired unknown (w/c ratio) by carrying out the most time-consuming phase (solution of the electromagnetic problem) during the training stage [21]. ANNs have successfully been applied to such diverse areas as speech and pattern recognition, financial and economic forecasting, telecommunications, and RF and microwave design [22]. Recently, they have also successfully been employed for various applications [21–27].

ANNs make possible to define the relation (linear or nonlinear) among a number of variables without knowledge of their cause-effect mechanisms. A multilayer perceptron (MLP) is composed of multiple neurons arranged in several different layers. The configuration of the best MLP model includes choosing the number of layers, the number of neurons in hidden layer, the activation function, the error function and the learning algorithm. After the proper architecture of the MLP has been established, all the training cases are run through the network. In each neuron, a linear combination of the weighted inputs (including a bias) is computed, summed and transformed using a transfer function (linear or nonlinear). The value obtained is passed on as an input to the neurons in the subsequent layer until a value is computed in neurons of the output layer. The output values are compared with the target outputs. The difference between the output and target is calculated using a certain error function in order to give the prediction error made by the network. Then, the training algorithm is used to adjust the network's weights and thresholds in order to minimize this error [28, 29].

In this study, we used free-space amplitude-only reflection and/or transmission measurements and time as inputs to ANN and w/c ratio as the output to ANN. Hyperbolic tangent function was used in hidden layer neurons, and logistic function was used in output layers. Networks were trained using the back-propagation algorithm. Weighted sums of the input components are calculated by using the following function

$$u_j = \sum_{i=1}^{n} w_{ij} x_i - b_j \tag{1}$$

where u_j is the weighted sum of the jth neuron for the input received from the preceding layer with n neurons, w_{ij} is the weight between the jth neuron and the ith neuron in the preceding layer, x_i is the output of the ith neuron in the preceding layer, and b_j is the bias of the jth neuron. The output of the jth neuron a_j in a hidden layer is calculated with a hyperbolic tangent function as

$$a_j = f(u_j) = \frac{\exp(u_j) - \exp(-u_j)}{\exp(u_j) + \exp(-u_j)}, \tag{2}$$

and the outputs of the output layer is calculated with a logistic function as

$$a_j = f(u_j) = \frac{1}{1 + \exp(-u_j)}. \tag{3}$$

The best network was searched using one hidden layer and two hidden layer network architectures. Levenberg-Marquardt optimization

technique was implemented for error minimization. To prevent
overfitting problems, an early-stopping technique is adopted. The
designed ANN consists of subdivided data sets in three subsets:
Training (approximately two thirds of total data), validation (one
sixth of total data) and test (one sixth of total data). We selected
the training, validation and test data from overall measurement data
randomly to minimize the overall fitting error. R^2 value of a model is
the proportion of the total variability in the dependent variable that is
accounted for by the model [30]. R^2 ($R^2 = 1$ for best matching) value
of the ANN model implies that the constructed neural network model
makes very close estimates for the observed values. After some trials,
we noted that 9 neurons in the hidden layer give optimum R^2 values.
For demonstration of this matching, we used the measured free-space
reflection and transmission properties of young mortar samples with
different w/c ratios in [15]. For example, Figs. 3 and 4 demonstrate
the estimated (output) w/c ratios of specimens over time for w/c ratios
varying from 0.40 to 0.60 with 0.05 increments using the data in Figs. 1
and 2. In addition, in Table 1, we illustrate the R^2 values of training,
validation, test and all measurement data.

It is seen from Figs. 3 and 4 and Table 1 that there is a good
fit between the measured data and the trained data by the designed
ANN. In addition, it is seen from Table 1 that, for w/c ratio estimation,
transmission and reflection measurements can be equally employed.
This shows the possibility of w/c ratio prediction from free-space
transmission measurements of young mortar specimens.

It is instructive to analyze which measurement parameters or
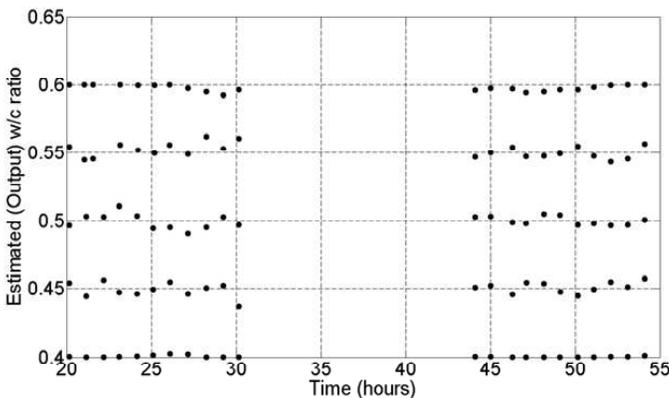data are key factors in the estimation of w/c ratio. For this reason,

Figure 3. Estimated (output) w/c ratio values using measured free-space reflection measurements in [15].
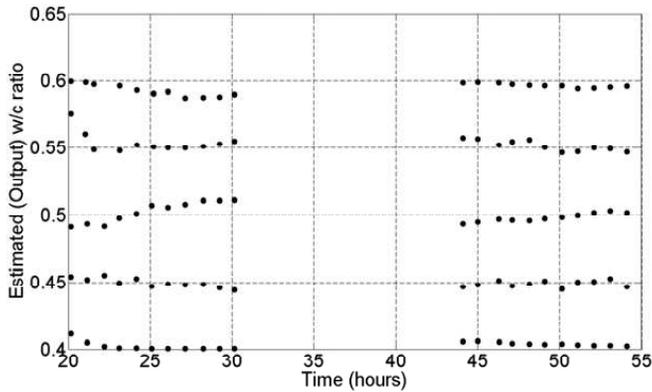
Figure 4. Estimated (output) w/c ratio values using measured free-space transmission measurements in [15].

Table 1. R^2 values of test, training, validation and all data of reflection or transmission measurements of young mortar specimens by the designed ANN.

	Reflection Measurement Data			
	Test	Training	Validation	All
R^2 value	0.994509	0.997823	0.994089	0.996675
	Transmission Measurement Data			
	Test	Training	Validation	All
R^2 value	0.996183	0.995061	0.98696	0.993889

Table 2. R^2 values of test data of reflection measurements of young mortar specimens after removal of data corresponding to each w/c ratio by the designed ANN.

	Removed data	R^2 value
	w/c = 0.40	0.994031
	w/c = 0.45	0.996549
Reflection Measurements	w/c = 0.50	0.999522
	w/c = 0.55	0.999642
	w/c = 0.60	0.999057

we trained the ANN by removing the reflection or transmission measurement data corresponding to each w/c ratio. Then, we compared the R^2 values of training data set after data removal. Table 2 demonstrates the effect of data removal of reflection measurement data.

It is seen from Table 2 that removing the measurement data with w/c ratio drastically alter the R^2 value while removal of others slightly changes R^2 value. This can be the effect of larger absolute temporal amplitude difference in reflection properties of mortar samples with w/c = 0.40 and w/c = 0.45 among the temporal differences of the remaining specimens [15]. Contrary to the effect of data removal from reflection measurements, we noted that removal of transmission data corresponding to each w/c had almost the same effect on R^2 value. This result is in good agreement with the measured transmission data in Fig. 2.

In order to estimate w/c ratios using reflection and transmission properties between 30 and 44 hours, we firstly interpolated these properties using measurements in Figs. 1 and 2. After interpolation, we applied our ANN to estimate the w/c ratio from measurements between 30 and 44 hours. Figs. 5 and 6 plot the estimated (output) w/c ratios of specimens over time for w/c ratios varying from 0.40 to 0.60 with 0.05 increments using the data in Figs. 1 and 2 after interpolation.

It is seen from Figs. 5 and 6 that there is good agreement with the expected w/c and the w/c of the trained ANN. As a result, one can employ the ANN for predicting the w/c ratio of materials from both reflection and transmission measurements over 20–55 hours.

Since we do not have extra measurement data of reflection and transmission measurement of samples with w/c ratios different than
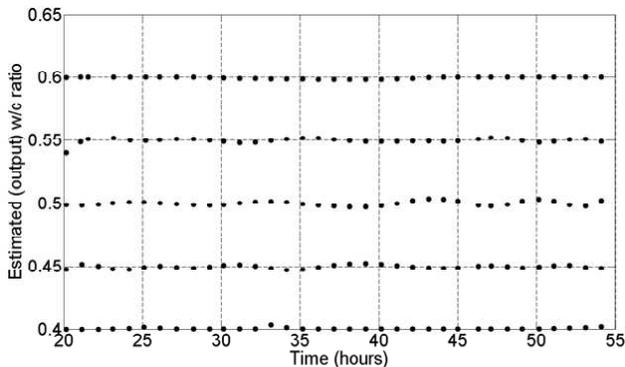

Figure 5. Estimated (output) w/c ratio values using measured free-space reflection measurements in [15] and interpolated data.
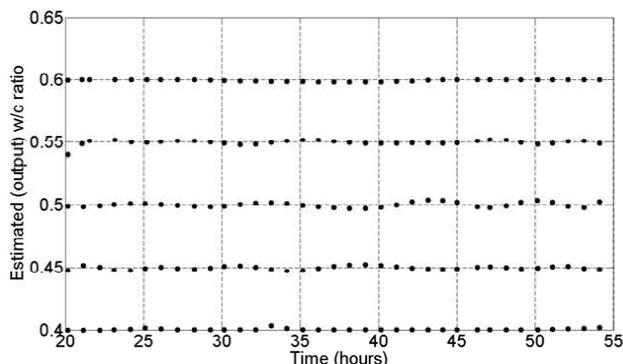
Figure 6. Estimated (output) w/c ratio values using measured free-space reflection measurements in [15] and interpolated data.
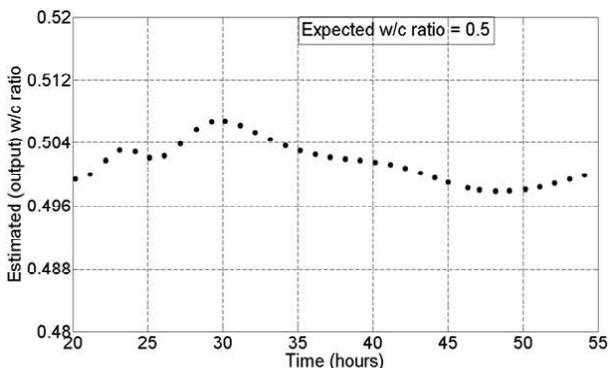

Figure 7. Estimated (output) w/c ratio versus time from the trained ANN using reflection measurements with (w/c = 0.40, 0.45, 0.55, 0.60) for estimating the w/c = 0.5.

those in Figs. 1 and 2, we could not directly test the trained ANN after interpolation. Instead, we removed the reflection and transmission measurement data with w/c ratio and tried to estimate it using the remaining data. For example, Fig. 7 demonstrates the accuracy of the trained ANN using reflection measurement data for estimation of w/c = 0.5.

It is seen from Fig. 7 that there is a good agreement with the output of the trained ANN and the expected w/c ratio (w/c = 0.5). We obtained a similar result shown in Fig. 7 using the same procedure applied for reflection measurements from transmission measurements. This clearly shows the applicability of the trained ANN for prediction of w/c ratio using free-space reflection and transmission measurements.

It has to be pointed out that the ANNs can process the entered or inputted data for evaluation or prediction of desired output. Not only vary the w/c ratios of cement-based materials with time due to water evaporation, hydration, etc, but also their electrical properties change over time with the actual water content and/or water-cement interaction. As a result, although the w/c ratio prediction by the employed ANN approach from measured free-field reflection and transmission measurements is suitable for time periods over 20–55 hours, it may not give accurate w/c estimation aside from these time periods. It is for this reason that to ensure a better w/c prediction using transmission and reflection measurements on samples at 30–44 hours by the employed ANN, real measurements can be utilized. Since this time period corresponds to night time, we could not conducted measurements over this period [15].

We also note that accuracy w/c ratio prediction of samples using reflection and transmission measurements by ANNs depends on how accurately these measurements are carried out. It is known that any misalignment of the aperture of sample (angle deviation) yields different free-space reflection and transmission properties, and reflection properties are affected much. As a result, transmission measurements may be more suitable for w/c prediction of cement-based materials by the ANNs if both sides of specimens are accessible. On the other hand, reflection measurements are more preferable if only one side of the specimens is reachable.

5. CONCLUSION

We have applied artificial neural networks (ANNs) for accurate prediction of the water-to-cement ratio (w/c) of cement based materials from free-space reflection and transmission measurements. This is important for w/c ratio estimation of cement-based materials since w/c ratio is the key factor affecting the strength of these materials most. We have trained the network from the previous free-space reflection and transmission measurements. After training the ANN, we have tested the network and observed that the trained ANN results are fairly accurate in w/c prediction.

with an outstanding young scientist award in electromagnetics for supporting his studies.

REFERENCES

1. Zoughi, R., *Microwave Non-destructive Testing and Evaluation*, Kluwer Academic Publishers, Dordrecht, The Netherlands, 2000.

2. Aydin, A. C., A. Arslan, and R. Gül, "Mesoscale simulation of cement based materials' time-dependent behavior," *Computational Materials Science*, Vol. 41, 20–26, 2007.

3. Bois, K. J., A. D. Benally, P. S. Nowak, and R. Zoughi, "Curestate monitoring and water-to-cement ratio determination of fresh Portland cement-based materials using near-field microwave techniques," *IEEE Trans. Instrum. Meas.*, Vol. 47, 628–637, 1998.

4. Neville, A. M., *Properties of Concrete*, Longman Group, London, UK, 1996.

5. Malhotra, V. M. and N. J. Carino (Eds.), *Handbook on Nondestructive Testing of Concrete*, CRC Press, Boca Raton, FL, 2004.

6. Zainud-Deen, S. H., M. E. S. Badr, E. El-Deen, and K. H. Awadalla, "Microstrip antenna with corrugated ground plane structure as a sensor for landmines detection," *Progress In Electromagnetics Research B*, Vol. 2, 259–278, 2008.

7. Yan, L. P., K. M. Huang, and C. J. Liu, "A noninvasive method for determining dielectric properties of layered tissues on human back," *Journal of Electromagnetic Waves and Applications*, Vol. 21, 1829–1843, 2007.

8. Zainud-Deen, S. H., W. M. Hassen, E. M. Ali, and K. H. Awadalla, "Breast cancer detection using a hybrid finite difference frequency domain and particle swarm optimization techniques," *Progress In Electromagnetics Research B*, Vol. 3, 35–46, 2008.

9. Zainud-Deen, S. H., M. E. S. Badr, E. El-Deen, K. H. Awadalla, and H. A. Sharshar, "Microstrip antenna with defected ground plane structure as a sensor for landmines detection," *Progress In Electromagnetics Research B*, Vol. 4, 27–39, 2008.

10. Capineri, L., D. Daniels, P. Falorni, O. Lopera, and C. Windsor, "Estimation of relative permittivity of shallow soils by using the ground penetrating radar response from different buried targets," *Progress In Electromagnetics Research Letters*, Vol. 2, 63–71, 2008.

11. Zhang, H., S. Y. Tan, and H. S. Tan, "An improved method for microwave nondestructive dielectric measurement of layered

media," *Progress In Electromagnetics Research B*, Vol. 10, 145–161, 2008.

12. Carriveau, G. W. and R. Zoughi, "Nondestructive evaluation and characterization of complex composite structures," *Proc. 11th Int. Symp. Nondestructive Characterization of Materials*, 273–280, Berlin, Germany, 2002.

13. Arunachalam, K., V. R. Melapudi, L. Udpa, and S. S. Udpa, "Microwave NDT of cement-based materials using far-field reflection coefficients," *NDT & E Int.*, Vol. 39, 585–593, 2006.

14. Bois, K. J., A. D. Benally, and R. Zoughi, "Microwave near-field reflection property analysis of concrete for material content determination," *IEEE Trans. Instrum. Meas.*, Vol. 49, 49–55, 2000.

15. Mubarak, K., K. J. Bois, and R. Zoughi, "A simple, robust, and on-site microwave technique for determining water-to-cement ratio (w/c) of fresh Portland cement-based materials," *IEEE Trans. Instrum. Meas.*, Vol. 50, 1255–1263, 2001.

16. Ganchev, S. I., S. Bakhtiari, and R. Zoughi, "A novel numerical technique for dielectric measurement of generally lossy dielectrics," *IEEE Trans. Instrum. Meas.*, Vol. 41, 361–365, 1992.

17. Pieraccini, M., G. Luzi, D. Mecatti, L. Noferini, and C. Atzeni, "A microwave radar technique for dynamic testing of large structures," *IEEE Trans. Microw. Theory Tech.*, Vol. 51, 1603–1609, 2003.

18. Arunachalam, K., V. R. Melapudi, E. J. Rothwell, L. Udpa, and S. S. Udpa, "Microwave NDE for reinforced concrete," *Review of progress in QNDE*, Vol. 25, 455–460, 2006.

19. Kharkovsky, S. N., M. F. Akay, U. C. Hasar, and C. D. Atis, "Measaurement and monitoring of microwave reflection and transmission properties of cement-based materials," *IEEE Trans. Instrum. Meas.*, Vol. 51, 1210–1218, 2002.

20. Kharkovsky, S. N. and C. D. Atis, "Nondestructive testing of mortar specimen by using the microwave free-space method," *J. Mater. Civ. Eng.*, Vol. 15, 200–204, 2003.

21. Hasar, U. C., "Free-space nondestructive characterization of young mortar samples," *J. Mater. Civ. Eng.*, Vol. 19, 674–682, 2007.

22. Hasar, U. C., "Non-destructive testing of hardened cement specimens at microwave frequencies using a simple free-space method," *NDT & E Int.*, Vol. 42, 550–557, 2009.

23. Trabelsi, S. and S. O. Nelson, "Free-space measurement of

dielectric properties of cereal grain and oilseed at microwave frequencies," *Meas. Sci. Technol.*, Vol. 14, 589–600, 2003.

24. ASTM, "Standart specification for concrete aggregates," *Annual Book of ASTM Standards, ASTM C-33*, West Conshohocken, Pa, 1990.

25. ASTM, "Standard test method for specific gravity and absorption of fine aggregate," *Annual Book of ASTM Standards*, ASTM C-128, West Conshohocken, Pa, 1993.

26. Ida, N., *Microwave NDT*, Kluwer Academic Publishers, Dordrecht, The Netherlands, 1992.

27. Olmi, R., G. Pelosi, C. Riminesi, and M. Tedesco, "A neural network approach to real-time dielectric characterization of materials," *Microwave Opt. Technol. Lett.*, Vol. 35, 463–465, 2002.

28. Zhang, Q. J. and K. C. Gupta, *Neural Networks for RF and Microwave Design*, Artech House, Norwood, MA, 2000.

29. Jargon, J. A., K. C. Gupta, and D. C. DeGroot, "Applications of artificial neural networks to RF and microwave measurements," *Int. J. RF and Microwave CAE*, Vol. 12, 3–24, 2002.

30. Guney, K., C. Yildiz, S. Kaya, and M. Turkmen, "Artificial neural networks for calculating the characteristic impedance of air-suspended trapezoidal and rectangular-shaped microshield lines," *Journal of Electromagnetic Waves and Applications*, Vol. 20, 1161–1174, 2006.

31. Jin, L., C. L. Ruan, and L. Y. Chun, "Design E-plane bandpass filter based on EM-ANN model," *Journal of Electromagnetic Waves and Applications*, Vol. 20, 1061–1069, 2006.

32. Mohamed, M. D. A., E. A. Soliman, and M. A. El-Gamal, "Optimization and characterization of electromagnetically coupled patch antennas using RBF neural networks," *Journal of Electromagnetic Waves and Applications*, Vol. 20, 1101–1114, 2006.

33. Ayestarn, R. G. and F. Las-Heras, "Near field to far field transformation using neural networks and source reconstruction," *Journal of Electromagnetic Waves and Applications*, Vol. 20, 2201–2213, 2006.

34. Ripley, B. D., *Pattern Recognition and Neural Networks*, Cambridge University Press, Cambridge, UK, 1996.

35. Haykin, S., *Neural Networks: A Comprehensive Foundation*, Macmillan College (IEEE Book Press), New York, NY, 1996.

36. Montgomery, D. C. and G. C. Runger, *Applied Statistics and Probability for Engineers*, Wiley, New Jersey, NJ, 2003.